Inelastic Scattering and Participating Media. Application to the Ocean.

E. Cerezo and F.J. Seron

Department of Computer Science, University of Zaragoza, Spain

Abstract

A system, developed to treat general participating media, is generalized to make it capable of considering volumetric inelastic processes such as fluorescence. The system is based on the discrete ordinates method, and can treat complex participating medium such as natural waters. It can deal with highly-peaked anisotropic phase functions and can handle the spectral behavior of the medium's characteristic parameters.The system is applied to the study of fluorescence, the most common inelastic effect in natural waters.

Categories and Subject Descriptors (according to ACM CCS): I.3.3 [Computer Graphics]: I.3.7 [Three-Dimensional Graphics and Realism]:

1. Previous work

The rendering of scenes containing participating media (such as water, clouds, smoke, fog...) has become increasingly widespread. Several methods have been developed to deal with these kind of scenes. In Table 1 the different methods and some relevant works are outlined. A good review of them and most relevant works can be found in[1]. Nevertheless, inelastic phenomena (with transfer of energy from one wavelength to another) are obviated in practically all global illumination systems. There are only two exceptions:

1. Glassner[21] was the first one, and till recently the only one, to consider fluorescence and phosphorescence when rendering scenes. His work focuses on the correct formulation of the rendering equation to include such effects. He also presents some results obtained with a public domain raytracer (Rayshade) adequately adapted. Anyway, when considering the more general case of scenes containing participating media, fluorescence is treated as a surface phenomenon. To deal with it, surfaces are characterized with a matrix that represents the transfer of energy from one wavelength to another one. As the transfer of energy, in most materials, is from large to small wavelengths the matrices are triangular. The visible spectrum is divided into intervals and a calculation is made for each of the wavelength values. In each of those calculations, energy in the smaller wavelengths is accumulated according to the surfaces' characteristic matrices. Before beginning a new wavelength calculation all objects of the scene are revised to select those with an appreciable emission to include them as sources in that calculation. This way, fluorescent energy is incorporated into the calculation.

Methods	*References*
Zonal	2 3 4 5 6
Spherical harmonics	7 8
Discrete Ordinates	9 10 11
Monte Carlo	12 13 14 15 16 17
Others	18 19 20

Table 1: *Different methods for participating media and some relevant works.*

2. Wilkie et al.[22] treat fluorescence in an analogous way. The originality of their work is that they are able to considered polarization and fluorescence simultaneously, two physical phenomena still rarely considered in current rendering systems. The fluorescence they consider is again surface fluorescence, produced by pigments. So, instead of characterizing the surfaces by means of the typical reflectance spectra, triangular re-radiation matrices are used. They use bispectral reflectivity values that are determined experimentally, but they exaggerate

them so that the effects are more visible in the scenes. They use a public domain raytracer (ART) developed in the Institute of Computer Graphics and Algorithms of the Vienna University of Technology.

It should be noted that in both cases fluorescence is treated as a *surface* phenomenon, whereas the aim of this work is to be able to deal with a fluorescence within a *volume*.

The structure of this paper is as follows: in Section 2 the usual radiative transfer equation (RTE) is generalized so that it is able to consider inelastic scattering. In Section 3 our general simulation system is outlined and the changes needed to be performed to the general discrete-ordinates calculation scheme to consider volumetric inelastic processes are discussed. Section 4 presents the oceanic medium as a participating medium, paying special attention to one of the naturally occurring inelastic processes: fluorescence. Section 5 includes the results and in Section 6 conclusions and future work are discussed.

2. Inelastic phenomena and participating media: the Full Radiative Transfer Equation

The equation that governs the transfer of energy when dealing with participating media[7] is the so-called Radiative Transfer Equation (RTE):

$$\frac{dL_\lambda(S,\theta,\varphi)}{dS} = -a_\lambda(S)L_\lambda(S,\theta,\varphi) + a_\lambda(S)L_{\lambda emis}(S,\theta,\varphi) - \sigma_\lambda(S)L_\lambda(S,\theta,\varphi) + \frac{dL_\lambda(S)}{4\pi}\int_{\omega_i=4\pi} L_{\lambda_i}(S,\theta_i,\varphi_i)\Phi(S,(\theta_i,\varphi_i)\rightarrow(\theta,\varphi))d\omega_i \quad (1)$$

This equation gives the local variation of the radiance when traversing a distance dS. The first term refers to absorption, where $a_\lambda(S)$ is the so-called absorption coefficient (the fraction of energy lost per unit length, dimension m^{-1}). The second term corresponds to self-emission, where $L_{\lambda emis}(S,\theta,\varphi)$ is the radiant energy emitted, due to spontaneous or stimulated emission. The third term represents the reduction of the radiance along the propagation direction because of scattering (out-scattering): $\sigma_\lambda(S)$ is the scattering coefficient (dimensions m^{-1}). The last term accounts for the in-scattering, ie, the increase of radiance along the propagation direction due to the scattering of radiance coming from other directions. $\Phi(S,(\theta_i,\varphi_i)\rightarrow(\theta,\varphi)$ is the phase function which describes the angular distribution of the scattered energy. In Table 2 the parameters characterising a participating medium are summarized. Their spectral dependence should be noted.

The extinction coefficient κ_λ, which is the sum of the absorption and scattering coefficients, is usually used to group the diminishment terms:

Symbol	*Meaning*
a_λ	Absorption coefficient (m^{-1})
σ_λ	Scattering coefficient (m^{-1})
κ_λ	Extinction coefficient (m^{-1})
$\Phi_\lambda(S,(\theta_i,\varphi_i)\rightarrow(\theta,\varphi))$	Phase function
$l_\lambda = 1/\kappa_\lambda$	Attenuation length (m)

Table 2: *Coefficients characterising a participating medium*

$$\frac{dL_\lambda(S,\theta,\varphi)}{dS} = a_\lambda(S)L_{\lambda emis}(S,\theta,\varphi) - \kappa_\lambda(S)L_\lambda(S,\theta,\varphi) + \frac{dL_\lambda(S)}{4\pi}\int_{\omega_i=4\pi} L_{\lambda_i}(S,\theta_i,\varphi_i)\Phi(S,(\theta_i,\varphi_i)\rightarrow(\theta,\varphi))d\omega_i \quad (2)$$

In fact, what is generally computed is not the radiance of the voxel for each direction but the *Source Term*, that represents the gain of radiance in one direction owing to in-scattering and emission:

$$G_\lambda(S,\theta,\varphi) = a_\lambda(S)L_{\lambda emis}(S,\theta,\varphi) + \frac{dL_\lambda(S)}{4\pi}\int_{\omega_i=4\pi} L_{\lambda_i}(S,\theta_i,\varphi_i)\Phi(S,(\theta_i,\varphi_i)\rightarrow(\theta,\varphi))d\omega_i \quad (3)$$

The RTE is valid only when elastic scattering occurs. But there are some physical phenomena that involve a transfer of energy from one wavelength to another. This is the case of fluorescence. To treat those phenomena, the RTE has to be generalized. Specifically, when considering in the in-scattering term the gain in the radiance in one specific direction and wavelength, not only must the transfers from other directions be considered but also the transfers from other wavelengths. So, the RTE has to be generalized to obtain the Full-Radiative Transfer Equation (FRTE):

$$\frac{dL_\lambda(S,\theta,\varphi)}{dS} = a_\lambda(S)L_{\lambda emis}(S,\theta,\varphi) - \kappa_\lambda(S)L_\lambda(S,\theta,\varphi) + \int_{\omega_i}\int_{R_v} F(S,\lambda_i\rightarrow\lambda,(\theta_i,\varphi_i)\rightarrow(\theta,\varphi))L_{\lambda_i}(S,\theta_i,\varphi_i)d\omega_i d\lambda_i \quad (4)$$

$F(S,\lambda_i\rightarrow\lambda),(\theta_i,\varphi_i)\rightarrow(\theta,\varphi))$ represents the probability that radiance in the (θ_i,φ_i) direction of wavelength λ_i gives rise to radiance of wavelength λ in the (θ,φ) direction. It will be, in general, the summation of the probability associated to each of the phenomena: elastic and inelastic. For elastic scattering:

$$F(S,\lambda_i \rightarrow \lambda,(\theta_i,\varphi_i) \rightarrow (\theta,\varphi)) \equiv$$

$$\frac{\sigma_{\text{elas}}(S,\lambda)}{4\pi}\Phi(S,(\theta_i,\varphi_i) \rightarrow (\theta,\varphi)) \quad (5)$$

and for the inelastic one, by analogy:

$$F(S,\lambda_i \rightarrow \lambda,(\theta_i,\varphi_i) \rightarrow (\theta,\varphi)) \equiv$$

$$\frac{\sigma_{\text{ine}}(S,\lambda_i \rightarrow \lambda)}{4\pi}\Phi(S,(\theta_i,\varphi_i) \rightarrow (\theta,\varphi)) \quad (6)$$

where σ_{ine} is the inelastic scattering coefficient (m^{-1}).

3. The CORDIS system

Due its complexity, when considering light transport in participating media, strong simplifications are usually made (single scattering, isotropic scattering, homogeneous media...). On the contrary, our CORDIS system focuses on the physical simulation of the transport of light in the more general case: non-homogeneous media, anisotropic scattering and multiscattering. It is specially well-suited to the consideration of complex participating media characterized by highly-peaked phase functions as well as to consider the spectral behavior of the medium characteristic parameters (Table 2). Besides the generation of synthetic images, the system generates detailed quantitative illumination information such as the amount of light that reaches the medium boundaries or the amount of light absorbed in each of the medium voxels. It is based on the work of Languénou et al.[11] that rests on the spatial discretization of the participating medium in finite volumes (voxels) and on the use the discrete ordinates method[23] to handle directions. Our main contribution to Languénou's method has been its generalization so that the system is able to:

- include objects (lambertian for the moment) and sources inside the participating medium
- use realistic spectral medium parametrizations
- handle highly anisotropic phase functions: besides the directions quadrature, additional characteristic directions can be added to handle peaks present in the medium phase function
- validate the results to assure that they are not only qualitatively but quantitatively (physically) correct: in particular the energies absorbed and scattered in each of the voxels are also calculated; this allows us to validate and estimate the accuracy of our calculation results by means of energy balances
- consider inelastic processes.

The work presented in this paper focuses on the fifth point. Our system has been presented elsewhere[24].

All the magnitudes in the simulations are treated as spectral ones: the source spectrum is divided into intervals, so that one calculation is carried out for each of the discrete wavelength values. The resolution method is iterative. First of all, an initialization step corresponding to the first order of scattering is performed. Then, in the iterative process, each of the iterations corresponds to one scattering. The results of this process are the source terms in each direction in each voxel of the medium, the outgoing radiances of the medium's boundaries and the irradiances in the surfaces within the medium. A simple ray-tracer adapted to voxelised media (TRAMPA) is used to obtain the images.

3.1. Adapting the system.

As stated in Section 1, practically all global illumination systems work by uncoupling wavelengths. The solution for the radiance corresponding to one wavelength is independent from the solution corresponding to another wavelength. This would be the case of the example shown in Figure 1, which corresponds to the first type of calculations carried out with our calculation system. For each of these calculations, one sets out from the participating medium with no previously calculated data (uncolored cube) and from the power emitted by the source/s in the wavelength of interest. The result of the calculation of that wavelength does not influence the results of other calculations in any way and is only used in the final rendering stage. However, the uncoupling cannot be carried out if inelastic phenomena have to be considered. In those cases, the transfer equation to be applied is the generalized one presented in Section 2. The energy transfers we are considering are always from high to low energies, or what amounts to the same thing, from smaller to larger wavelengths. This makes it necessary to carry out the successive spectral calculations in the order of increasing wavelengths. As shown in Figure 2, the results obtained in the calculation of one wavelength influence the calculations corresponding to all the subsequent wavelengths. Thus, when initiating the calculation corresponding to the first wavelength (the smaller one) the medium is void of data (black cube). This is why in this case, the energy emitted by the source is taken as the only input. The output of the calculation is the medium calculated for that wavelength (colored cube) but in addition, part of that energy has been transferred to higher wavelengths. As a result, when beginning the calculation for all other wavelengths the medium is not void, but contains energy corresponding to that wavelength originated in all previous calculations (colored cube). Thus, the energy emitted by the sources has to be added to that transferred energy. Once all the calculations have been made, the ray-tracer (TRAMPA) is used to obtain the colored image.

The consideration of inelastic processes makes it necessary to introduce certain changes in the general simulation scheme, in particular when dealing with the source terms.

1. Now, in addition to the elastic source terms in each dis-

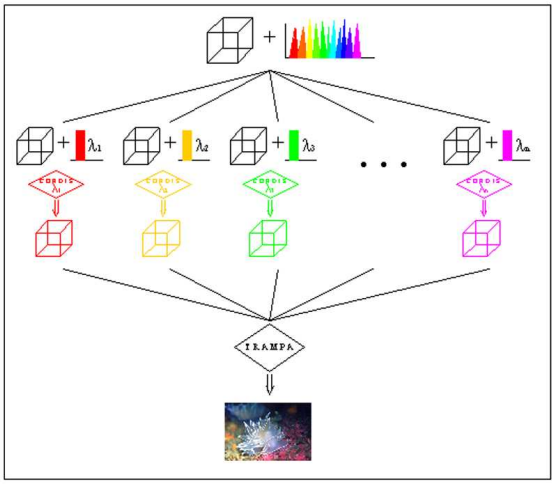

Figure 1: *Calculation when only elastic phenomena are taken into account.*

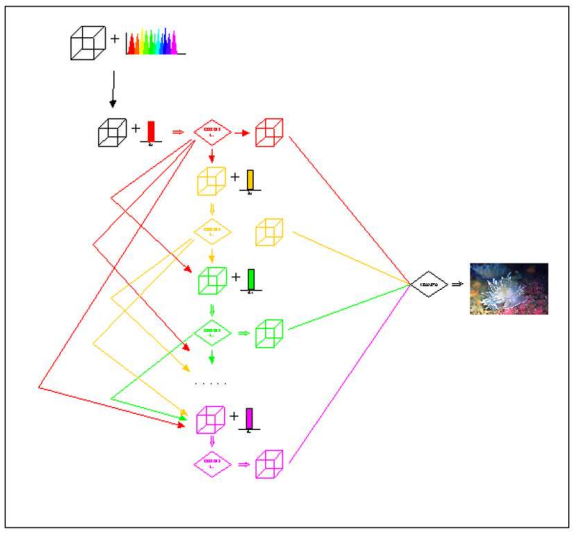

Figure 2: *Calculation in the case of taking both elastic and inelastic phenomena into account.*

crete direction, new inelastic source terms have to be stored in each voxel. These inelastic terms serve the purpose of accumulating the contributions coming from all the inelastic scattering taking place inside the voxel. If the inelastic phenomenon to be considered is isotropic, instead of storing one inelastic source term for each wavelength and each discrete direction, it is sufficient to store one single term for each calculation wavelength.

2. Now, when calculating the new orders of scattering in each voxel, the increment in the new inelastic source terms have to be computed from:

$$\Delta G_{ine}(\lambda,\theta,\varphi) = \sigma_{ine}(\lambda_i \rightarrow \lambda) w_i L_i(\lambda_i,\theta_i,\varphi_i) \quad (7)$$

where σ_{ine} is a generic inelastic scattering coefficient and ΔG_{ine} represents the increment in the source term corresponding to the discrete direction (θ,φ) and wavelength λ due to inelastic scattering of radiance in the (θ,φ) direction and wavelength λ_i ($\lambda > \lambda_i$).

3. In the inelastic case, when beginning the calculation of a new wavelength, the voxels' source terms in the discrete directions will not be zero (except in the case of the smaller wavelength, recall Figure 2): they would have to be initialized with the inelastic increments accumulated during the calculations corresponding to smaller wavelengths. Therefore, the source terms' initial values (before considering the emission of the light sources in that particular wavelength) will be (in the case of isotropic inelastic scattering):

$$G(\lambda,\theta,\varphi) = \frac{G_{ine}(\lambda)}{4\pi} \quad (8)$$

where G_{ine} contains the source terms contributions from all smaller wavelengths.

Calculation time depends mostly on the number of voxels (Figure 3) and is practically not affected by the above mentioned changes. On the contrary, memory requirements rise when considering inelastic effects. Our calculation method is memory consuming per se (3N + 3 real numbers are stored in each voxel, where N is the number of discrete directions). The increase in memory is because, as explained above, a new vector has to be saved in each voxel. This new vector is used to accumulate the inelastic light transfers corresponding to each discrete wavelength.

4. The participating medium: the ocean

The interesting issue about natural waters and, in particular, about the oceanic medium, is that electromagnetic radiation interacts not only with the water but with materials dissolved or suspended in it (dissolved salts, dissolved organic compounds- the so-called yellow matter or CDOM-, plankton...). This makes the ocean phenomenologically rich[26]. In fact, oceanic medium can be viewed just as a participating medium: light is scattered and absorbed as it trav-

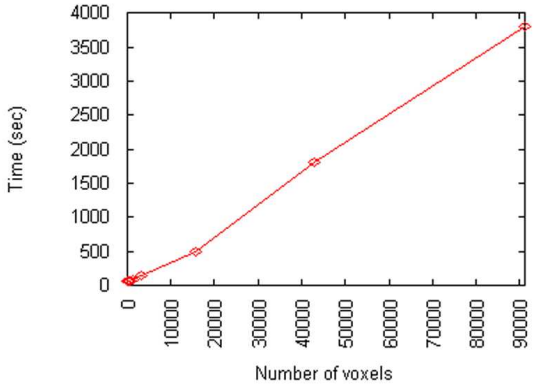

Figure 3: *Evolution of the calculation time when increasing the number of voxels (Pentium IV 1.7 GHz).*

els through the water. With respect to absorption, water is nearly "opaque" outside the wavelength range comprised between 400 and 700 nm. For elastic scattering, the substances present in the water increases the scattering coefficient by at least a factor of ten, and the phase function becomes highly peaked (Figure 4). In terms of inelastic scattering, fluorescence is a phenomenon of considerable significance in natural waters. Fluorescence occurs when a molecule absorbs an incident photon and shortly thereafter emits (between 10^{-8} and 10^{-11}s later) a photon of greater wavelength. Re-emission is not directional but isotropic. Fluorescence occurs in many substances present in natural waters. The most thoroughly studied is chlorophyll, but other pigments found in living phytoplankton or in yellow matter (CDOM), as well as hydrocarbons and other pollutants, often exhibit strong fluorescence.

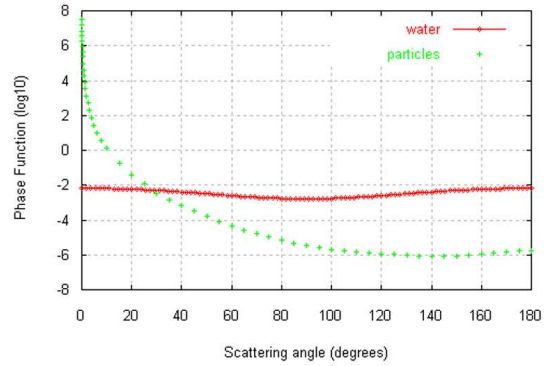

Figure 4: *Phase function owing to particles present in natural waters (green) compared to the pure water phase function (red).*

In the case of fluorescence, the inelastic scattering coefficient (Equation 6) is usually expressed[27]:

$$\sigma_{\text{ine}}(S,\lambda_i \rightarrow \lambda) \equiv a_{\lambda_i}(S) f_{\text{f}}(S,\lambda_i \rightarrow \lambda) = a_{\lambda_i}(S)\eta_{\text{f}}(S,\lambda_i \rightarrow \lambda)\frac{\lambda_i}{\lambda}d\lambda \quad (9)$$

where $a_{\text{f}}(S,\lambda_i)$ is the absorption coefficient (absorption of light is necessary so that fluorescent radiation can be emitted) and $f_{\text{f}}(S,\lambda_i \rightarrow \lambda)$ the fluorescent wavelength redistribution function. The $\eta_{\text{f}}(S,\lambda_i \rightarrow \lambda)$ is its quantum equivalent, the spectral fluorescence quantum efficiency function. A useful related quantity is the total fluorescence quantum efficiency:

$$\Gamma_{\text{f}} = \int_0^\infty \eta_{\text{f}}(S,\lambda_i \rightarrow \lambda)d\lambda \quad (10)$$

Γ_{f} determines the amount of re-emission since it is the quotient between the number of photons emitted in all wavelengths and the number of photons absorbed at the excitation wavelength.

5. Results

5.1. Test scene configuration

We have applied our resolution module to a simple test scene to study the incidence of fluorescence in the simulations. We have studied waters with high concentrations of biogenic constituents, that is to say, waters with highly scattering and extinction coefficients, and therefore, very limited visibility conditions. The considered extinction coefficients range from around 2m^{-1} to 5m^{-1} which implies attenuation lengths (Table 2) ranging from 2.5m to 0.33m. It is commonly assumed that visibility extends to no more than one or two attenuation lengths. Taking all this into account, we have worked with a calculation volume of 1m x 1m x 1m, subdivided into 25x25x25 voxels. The calculation volume is placed on the seabed around the object. It is assumed that the seabed is deep enough so that neither natural illumination nor the air-water surface boundary are considered. Therefore, the calculation volume is limited by two physical boundaries: a sandy seabed, with a plastic object placed on it, and a rocky vegetal wall at the back of the scene, all three (seabed, object and wall) characterized with their corresponding reflection coefficients. The scene is illuminated by an artificial incandescent isotropic source placed on top of the calculation volume pointing to the object. The camera is positioned outside the scene at a distance of 0.5m from the cube looking at its center (see Figure 5). A uniform quadrature of 74 directions (plus one characteristic direction in each voxel to account for the phase function peak) has been used. In order to account for the wavelength dependence of the final color image, the visible spectrum is divided up into

16 values that range from 400 to 700 nm in 20 nm increments. The 20nm sampling has been chosen due to the spectral properties of the scenes (no sharp color variations) and of the medium characteristic parameters but, more in depth studies should be performed[28, 29].

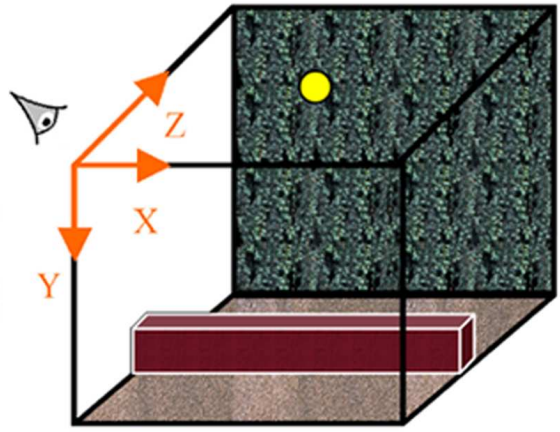

Figure 5: *Scene configuration.*

5.2. Fluorescence in pure substances (clorophyll-a)

A characteristic of fluorescence in pure substances is that the emission wavelengths are independent of the excitation wavelengths. Chlorophyll-a (the most abundant type of chlorophyll) always fluoresces in the band centered at 685 nm, regardless of whether it is excited by light at near ultraviolet, blue, green, or even red wavelengths. Therefore, in the case of chlorophyll-a, the calculation is simplified. The quantum efficiency, Γ_f, in this case ranges from 0.01 to 0.10 with typical values between 0.01 and 0.05 (most of the absorbed radiation will be released as heat).

We have chosen seawater with a high chlorophyll concentration (10 mg/m^3) characterized by parameters shown at the top of Figure 6. These parameters are realistic and obtained from bio-optical models[25]. As shown, scattering is so high that visibility is almost totally lost. Two situations have been compared: one which takes fluorescence into account (inelastic case) and one which does not (elastic case). Due to the fact that the increment takes place only in one of the wavelengths, no visible differences exist between the images generated in each case (even at higher chlorophyll concentrations). But there are quantitative differences. The energy absorbed in every wavelength in the water body is shown in Figure 7. As can be appreciated, the energy absorbed in the elastic case is always greater than in the inelastic case, because part of the absorbed energy is re-emitted. On the contrary, in the area of 680nm, the situation is reversed. This is because this wavelength is the only one that receives energy from all the other wavelengths. A quantum efficiency Γ_f of 0.1 has been considered.

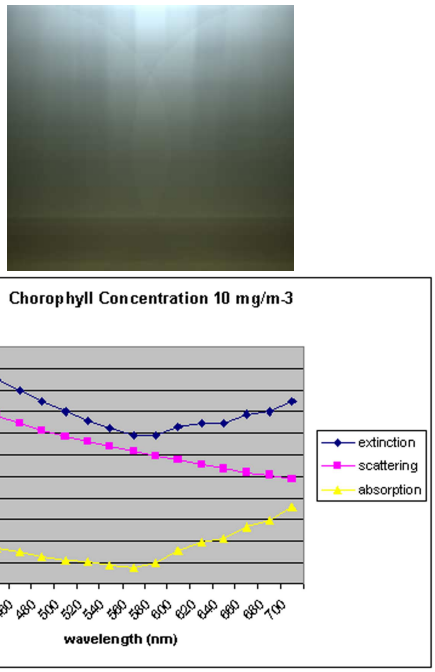

Figure 6: *Water body with high biogenic content (top). Characteristic parameters used in the simulation (bottom).*

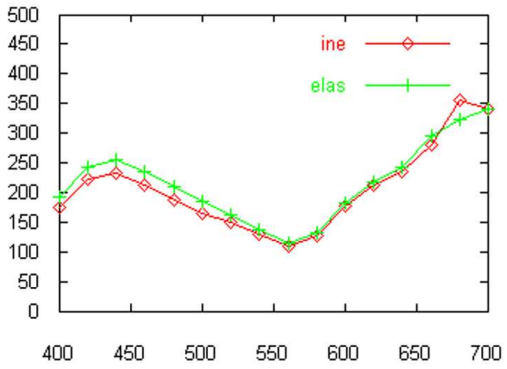

Figure 7: *Total energy absorbed in the medium whether considering fluorescence in chlorophyll-a (red)or not (green).*

5.3. Fluorescence in compounds (CDOM)

In the case of CDOM, fluorescence is more complicated and the calculation is of the type shown in Figure 2. The redistribution function, f_f, has to be appropriately normalized so that the energy conservation is maintained when transferring energy from one wavelength to another.The values of Γ_f generally fall between 0.005 y 0.015.

Figure 8 shows two images of the same test scene where fluorescence has been taken into account (left image) or not (right image). A quantum efficiency of 0.015 has been used. As opposed to the results presented in the previous section, differences are now visible.

Figure 8: *Images obtained considering fluorescence in CDOM (left) or not (right).*

6. Conclusions and future work

We have extended the radiative transfer equation to deal with inelastic phenomena when dealing with participating media. We have generalized a simulation system based on the discrete ordinates method so that it is able to incorporate the new kind of phenomena in the iterative calculation scheme. All these have allowed us to treat the most common inelastic phenomenon in natural waters: fluorescence. Realistic values of the medium parameters have been used throughout. Even in cases where there are no visible differences, quantitative results reveal the variation in the distribution of light in the media when considering fluorescence.

Related to future work, we are working in the integration of the CORDIS system in the global illumination system ALEPH[30] developed in our group, so that more complex and visually pleasant scenes can be considered.

On the other hand, our simulation system is not only capable of generating images but also quantitative illumination results. It should be noted that the resolution of the transport problem in the water is a prerequisite for the solution of many problems such as the synthesis of realistic underwater images, the underwater visibility, the capture of satellite images, the biologic productivity studies, or the thermodynamics of stratified media in submarine environments.

Acknowledgements

This work has been partly financed by the Spanish "Comisión Interministerial de Ciencia y Tecnología" (contracts number TIC2000-0426-P4-02 and TIC2001-2392-C03-02).

References

1. F. Pérez, X. Pueyo, F.X. Sillion. Global Illumination Techniques for the Simulation of Participating Media. *Proceedings of the Eight Eurographics Workshop on Rendering, Saint Etienne, France* Springer Verlag: 309-320, 1997 1

2. H.E. Rushmeier, K.E. Torrance. The Zonal Method for Calculating Light Intensities in the Presence of a Participating Medium. *Computer Graphics (ACM SIGGRAPH '87 Proceedings)*, **21(4)**: 293-302, 1987 1

3. N. Bhate. Application of Rapid Hierarchical Radiosity to Participating Media. Proceedings of ATARV-93: Advanced Techniques in Animation, Rendering, and Visualization: 43-53, 1993 1

4. F. Sillion. A Unified Hierarchical Algorithm for Global Illumination with Scattering Volumes and Object Clusters. *IEEE Transactions on Visualization and Computer Graphics* **1(3)**: 240-254, 1995 1

5. D. Arquès, S. Michelin. Proximity Radiosity: Exploiting Coherence to Accelerate Form Factor Computations. Rendering Techniques '96 (Proceedings of the Seventh Eurographics Workshop on Rendering): 143-152, 1996 1

6. F. Pérez, I. Martín, F.X. Sillion, X. Pueyo. Acceleration of Monte Carlo Path Tracing in General Environments. Proceedings of Pacific Graphics 2000, 2000 1

7. J.T. Kajiya, B.P. von Herzen. Ray-tracing volume densities. *Computer Graphics* **18(3)**: 165-174, 1984 1, 2

8. N. Bhate, A. Tokuta. Photorealistic Volume Rendering of Media with Directional Scattering. Third Eurographics Workshop on Rendering: 227-245, 1992 1

9. C. Patmore. Simulated Multiple Scattering for Cloud Rendering. Graphics, Design and Visualization (IFIP Transactions B-9): 59-70, 1993 1

10. N.L. Max. Efficient Light Propagation for Multiple Anisotropic Volume Scattering. Fifth Eurographics Workshop on Rendering: 87-104, 1994 1

11. E. Languènou, K. Bouatoch, M. Chellem. Global Illumination in Presence of Participating Media with General Properties. *In Photorealistic Rendering Techniques, Sakas, Shirley, Müller (eds.)* Springer Verlag: 71-86, 1995 1, 3

12. S.N. Pattanaik, S.P. Mudur. Computation of Global Illumination in a Participating Medium by Monte Carlo Simulation. *The Journal of Visualization and Computer Animation* **4(3)**: 133-152, 1993 1

13. P. Blasi, B. Le Saëc, C. Schlick. A Rendering Algorithm for Discrete Volume Density Objects. *Computer Graphics Forum* **12(3)**: C201-C210, 1993 1

14. P. Blasi, B. Le Saëc, C. Schlick. An Importance Driven Monte-Carlo Solution to the Global Illumination Problem. Fifth Eurographics Workshop on Rendering: 173-183, 1994 1

15. E.P. Lafortune, Y.D. Willems. Rendering Participating Media with Bidirectional Path Tracing. Rendering Techniques '96 (Proceedings of the Seventh Eurographics Workshop on Rendering: 91-100. Springer-Verlag/Wien, 1996 1

16. H. Wann Jensen, P.H. Christensen. Efficient Simulation of Light Transport in Scenes with Participating Media Using Photon Maps. Computer Graphics (ACM SIGGRAPH '98 Proceedings): 311-320, 1998 1

17. M. Pauly, T. Kollig, A. Keller. Metropolis Light Transport for Participating Media. Rendering Techniques 2000 (Proceedings of the Eleventh Eurographics Workshop on Rendering): 11-22. Springer Wien, 2000 1

18. T. Nishita, Y. Dobashi, E. Nakamae. Display of Clouds Taking Into Account Multiple Anisotropic Scattering and Sky Light. Computer Graphics Proceedings, Annual Conference Series (ACM SIGGRAPH '96 Proceedings): 379-386, 1996 1

19. J. Stam. Multiple Scattering as a Diffusion Process. Eurographics Workshop on Rendering 1995: 41-50, 1995 1

20. J. Stam, E. Fiume. Turbulent Wind Fields for Gaseous Phenomena. Computer Graphics Proceedings (ACM SIGGRAPH '93 Proceedings): 369-376, 1993 1

21. A. Glassner. A model for Fluorescence and Phosphorescence. *In Photorealistic Rendering Techniques, Sakas, Shirley, Müller (eds.)*, Springer Verlag **18**: 60-70, 1995 1

22. A. Wilkie, R.F. Tobler, W. Purgathofer. Combined Rendering of Polarization and Fluorescence Effects. *In Rendering Techniques'01 (Proc. Eurographics Workshop on Rendering 2001), Wien, June 2001; Gortler S. J., Myszkowski K. (eds.)*, Springer Verlag **18**: 197-204, 2001 1

23. H. Siegel, J.R. Howel. *Thermal Radiation Heat Transfer, Third edition.* Hemisphere Publishing Corporation, 1992 3

24. E. Cerezo, F.J. Serón. An Approach to the Simulation of the Sea as Participating Medium. *Computer & Graphics* **24(7)**, 2003 (*to appear*) 3

25. E. Cerezo, F.J.Serón. Rendering Natural Waters: Merging Computer Graphics with Physics and Biology. Proc. of the Computer Graphics International Conference 2002, Bradford: 481-498, 2002 6

26. R.W. Spinrad, K.L. Carder, M.J. Perry (eds.). *Ocean Optics, Oxford Monographs on Geology and Geophysics. Oxford University Press*, 1994 4

27. C.D. Mobley. *Light and water: Radiative Transfer in Natural Waters*. Academic Press, 1994 5

28. Y. Sun, F. Fracchia, M. Drew, T.Calvert. A spectrally based framework for realistic image synthesis. *The Visual Computer* **17(7)**, 2001 6

29. R. Hall. Comparing spectral computation methods. *IEEE Computer Graphics & Applications* **19(4)**, 1999 6

30. *The ALEPH system*. http://giga.cps.unizar.es/aleph-whatis.html. 7